ELSEVIER

Journal of Organometallic Chemistry 661 (2002) 191–197

Journal of Organometallic Chemistry

www.elsevier.com/locate/jorganchem

# Time-resolved photoelectron spectroscopy: A unique tool to monitor the vibrational and fragmentation dynamics of metal carbonyls

M. Erdmann [a], O. Rubner [b], Z. Shen [c], V. Engel [a,*]

[a] Institut für Physikalische Chemie, Universität Würzburg, Am Hubland, D-97074 Würzburg, Germany
[b] Institut für Nanotechnologie, Forschungszentrum Karlsruhe GmbH, Postfach 3640, D-76021 Karlsruhe, Germany
[c] Department of Chemistry, Princeton University, Princeton, NJ 08542, USA

Received 29 April 2002; accepted 2 July 2002

Dedicated to Professor Helmut Werner on the occasion of his retirement and in recognition of his tremendous contributions to organometallic chemistry

**Abstract**

We present simulations of time- and energy-resolved ionization experiments on iron carbonyls. In calculating photoelectron spectra we show that it is possible to track the temporal variation of a metal–carbon bond. As another example, the multiple CO abstraction from iron pentacarbonyl induced by multi-photon absorption is regarded. Here the time-dependence of photoelectron spectra as obtained from a pump–probe arrangement gives a unique picture of the fragmentation within the neutral manifold of $Fe(CO)_n$ molecules.


*Keywords:* Photoelectron spectroscopy; Iron carbonyls

## 1. Introduction

Taking early experimental observations into account, Einstein, in 1905, offered the first explanation for the photo-electric effect: the interaction of a solid with radiation of high enough frequency induces the emission of electrons which emerge with different kinetic energies. Einstein's equation

$$\frac{1}{2} m v_{\max}^2 = h\nu - I, \tag{1}$$

tells us that the maximum kinetic energy of the ejected electrons is determined by the difference between the photon energy ($h$ being Planck's constant, $\nu$ the frequency) and a minimum energy $I$, which in the case of a molecule is the ionization potential. This discovery was one of the first steps towards the development of quantum mechanics. Ever since, photoelectron spectroscopy (PES) has been applied to solid state systems and gas-phase molecules. The interaction of UV radiation with molecules leads to the removal of valence electrons thus yielding information about the binding properties of the neutral molecules and, additionally, the structure of the cations [1,2]. On the other hand, ionization triggered by X-ray sources prepares, a core hole which then leads to photon emission, Auger decay and related phenomena [3]. Still to be investigated is the inner valence shell ionization which should exhibit exciting new processes, like interatomic Coulomb decay (ICD) as predicted by recent theoretical studies [4].

It is possible to employ sub-picosecond laser pulses to initiate and probe the nuclear dynamics occurring in gas-phase or solvated molecules [5–8]. The scheme of these experiments can be summarized as follows: a first ultrashort laser pulse prepares the ensemble of molecules under consideration in a non-stationary state. This simply means that any measurement results in a time-

* Corresponding author. Tel.: +49-931-8886376; fax: +49-931-8886362
*E-mail address:* voen@phys-chemie.uni-wuerzburg.de (V. Engel).

0022-328X/02/$ - see front matter 
PII: S0022-328X(02)01822-3

dependent signal—provided one is able to set up an apparatus with a response time fast enough to resolve the temporal changes induced in the sample [9]. This indeed is feasible if one uses a pump–probe set up where a second ultrafast pulse (probe-pulse) is time-delayed with respect to the pump via a Michelson arrangement. The response of the system is then measured as a function of the pump–probe delay time.

Naturally, we may think of combining a time-resolved measurement with PES. This was suggested by Seel and Domcke in a seminal theoretical paper on the vibronic-coupling dynamics in pyrazine [10,11]. The idea was first realized experimentally by Cyr and Hayden [12] and, by now, several groups have performed measurements which proved the capability of time-resolved photoelectron spectroscopy (TRPES) to provide a deeper insight into dynamical processes occurring in molecules [13–22]. Recently, much effort has been put into the measurement of photoelectron distributions being detected not only as a function of time and energy, but also as a function of angular variables [23–25]. For example, Hayden and co-workers investigated the time-evolution of photoelectron angular distributions (PADs) during the femtosecond induced photodissociation of $NO_2$ [24]. In this way, it was possible to monitor the orientation of photofragments in real time. Theoretically, time-dependent PADs have been obtained in the groups of Seideman [26,27] and McKoy [28,29].

Even though several femtosecond time-resolved measurements on metal carbonyls have been performed [30–39], no experiment using TRPES has been carried out on these molecules. In this paper, we will discuss the application of TRPES to metal carbonyls in the gas-phase and in particular, iron carbonyls are treated. After outlining the theoretical background necessary to understand TRPES in Section 2, we present results on the vibrational dynamics of FeCO in Section 3. Section 4 discusses the multiple fragmentation of $Fe(CO)_5$. Finally, Section 5 presents a short summary.

## 2. The principle of time-resolved photoelectron spectroscopy

In conventional PES, the interaction-time of the external field with the system is much longer than the internal time-scales of the vibrational and rotational motion. The latter can be estimated from the separation of two adjacent eigenenergies $\Delta\varepsilon$ as

$$T = \frac{h}{\Delta\varepsilon}. \tag{2}$$

Regard the FeCO molecule as an example: here the vibrational wave-numbers are 530 (FeC) [40], 1946 (CO) [41] and 330 $cm^{-1}$ (bending) [40] which corresponds to times $T_{vib}$ of 62, 17 and 100 fs, respectively. The rotational period for the $J'' = 25 \leftarrow J'' = 24$ transition is about 4.7 ps [42]. Thus we see that a laser pulse with a temporal width of about 30 fs can be regarded as short compared to the time scale of the FeC and the bending vibrational motion and also the rotational motion. Since such a short pulse has a broad distribution of frequencies, the interaction of a molecule with the electromagnetic field results in the simultaneous excitation of several eigenstates $\varphi_n$. The time-dependent state $\psi(t)$ of the system then can be written as (atomic units are employed, $\hbar = 1$):

$$\psi(t) = \sum_n a_n \, e^{-i\varepsilon_n t} \, \varphi_n, \tag{3}$$

where $\varepsilon_n$ are the eigenenergies of the molecule and $a_n$ are coefficients which depend on the particular excitation process. The wave packet (Eq. (3)) is non-stationary, i.e. the probability density $|\psi(\boldsymbol{R}, t)|^2$, where $\boldsymbol{R}$ represents the vector of all atomic coordinates, changes with time, as will be illustrated in Section 3.

Suppose now, that a second ultrashort laser pulse, delayed with respect to the first one by time $T$, ionizes the molecule, yielding photoelectrons of kinetic energy $E$ and cations. In general, the outcome of the ionization process depends crucially on the time-delay between the first laser pulse (the pump-pulse) which prepares the wave packet and the second pulse (the probe-pulse). This can be shown using time-dependent perturbation theory, see for example, Ref. [43]. Here we only give the result which expresses the photoelectron spectrum (that is, the kinetic energy distribution of the ejected electrons) approximately as

$$P(E, \tau) \sim |\psi(\boldsymbol{R}, \tau)|^2. \tag{4}$$

The latter equation establishes a direct relationship between the photoelectron spectrum and the coordinate-dependent probability density. This relationship follows directly from the energy conservation law which is demonstrated in Fig. 1. At every point in space, the difference of the potential energy of the cationic state $V_+(\boldsymbol{R})$ and the neutral state $V_1(\boldsymbol{R})$ plus the energy of the electron must equal the carrier frequency $\omega_2$ of the probe-pulse:

$$\omega_2 = V_+(\boldsymbol{R}) - V_1(\boldsymbol{R}) + E. \tag{5}$$

The prepared wave packet (in the electronic state (Eq. (1)) changes its location in time. At the delay-time $T$, the probe-pulse starts the ionization process. The wave packet at time $T_1$ is centered around the minimum of the potential curve $V_1$. This position does not change substantially during the ionization process ($\omega_2$) which yields photoelectrons emerging most probably with energy $E$. The length of the downward pointing arrow corresponds to the energy $E$ as defined by the resonance condition (Eq. (5)). In the course of time, the wave

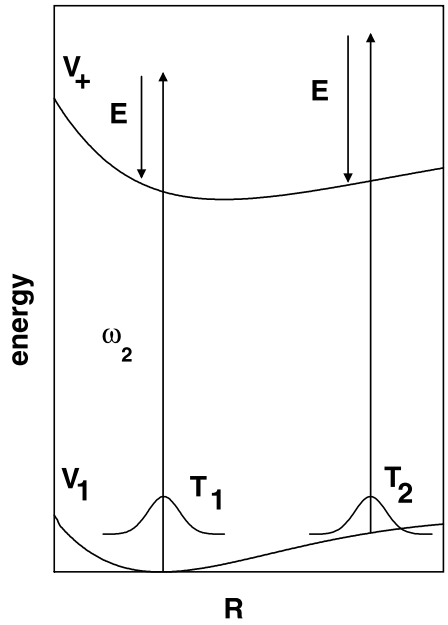


Fig. 1. The principle of TRPES: shown are wave packets $|\psi_1(\boldsymbol{R}, T)|^2$ at two different times $T_1$, $T_2$ in an electronic state (Eq. (1)) of a neutral molecule. Ionization as induced by a femtosecond laser pulse ($\omega_2$) results in photoelectrons with small ($T_1$) and large ($T_2$) kinetic energies, as is illuistrated by the length of the downward pointing arrows.

packet eventually reaches the outer potential wall at time $T_2$. Since now the potential difference $V_+(\boldsymbol{R})-V_1(\boldsymbol{R})$ at the wave packet's position is smaller compared to that at $T_1$, photoelectrons acquire more excess energy.

The discussion above shows that the temporal changes of a photoelectron spectrum, as recorded in a pump–probe experiment, is able to determine structural changes in a molecule. Even more intriguing, it is possible to monitor the time-evolution of the probability density of a wave packet prepared by a femtosecond excitation. To illustrate this principle we will treat the simple vibrational motion of the FeCO molecule in Section 3.

## 3. Vibrational dynamics of a single metal–carbon bond

In what follows we regard the vibrational wave-packet motion in the electronic triplet state $^3\Sigma^-$ [44] of FeCO. Within the laser-excitation processes treated here, the bending degree-of-freedom is not excited thus we confine the vibrational motion to the collinear configuration. Furthermore, the large frequency mismatch between the Fe–C and CO vibrations allows for an adiabatic separation between these modes. Therefore, only the Fe–C vibration is considered explicitly here, the CO distance is fixed at its equilibrium distance. Our example starts with the $FeCO^-$ anion (in its $^4\Sigma^-$ state [44]) and consists of two steps: an electron detachment, followed by an ionization process. Details of the theoretical treatment of the so-called NeNePo (negative-ion-to-neutral-to-positive-ion) process [45] can be found elsewhere [46].

The pump laser-pulse $W_1(\omega_1)$ (with a carrier frequency $\omega_1$ corresponding to 2.54 eV) initiates the following process:

$$FeCO^-(^4\Sigma^-) + W_1(\omega_1) \rightarrow FeCO(^3\Sigma^-) + e^-(E_1), \qquad (6)$$

where $e^-(E_1)$ is a photoelectron with energy $E_1$ originating from the detachment process. The pump process produces neutral molecules in non-stationary states. In fact, an entire manifold of wave packets has to be considered which differ with respect to the energy of the ejected electron as produced in coincidence [46]. Here we restrict our considerations to a particular energy of $E_1 = 1.34$ eV which corresponds to the maximum of the detachment spectrum. The nuclear wave-packet motion in the $^3\Sigma^-$ state of FeCO is displayed in Fig. 2. The probability density $|\psi(\boldsymbol{R}, t)|^2$ is shown as a function of the Fe–C bondlength and the time after the pump excitation. A Gaussian-like distribution is found which changes its mean position periodically. This is very close to our classical expectation of how a vibrational motion takes place. The quantum mechanical interpretation here is that at one time the entire ensemble of molecules which have been subject to the interaction with the first laser pulse, posses a maximum iron–carbon distance. Then, after an interval of about 30 fs the bondlength has reached a minimum value. This stretching and contracting of the bond then recurs with the vibrational period of ca. 60 fs.

We next turn to the probe process, where a second femtosecond pulse $W_2(\omega_2, T)$ with carrier frequency $\omega_2$ ($=9.5$ eV) and a time-delay $T$ interacts with the molecules and initiates the ionization process

$$FeCO(^3\Sigma^-) + W_2(\omega_2, T) \rightarrow FeCO^+(^4\Sigma^-) + e^-(E_2). \qquad (7)$$

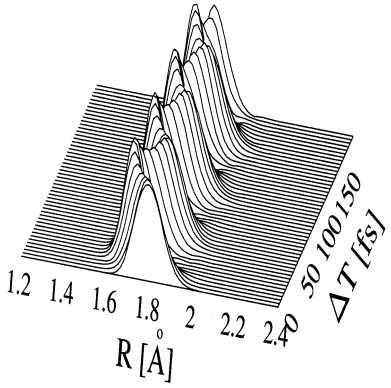


Fig. 2. Vibrational wave-packet motion within the FeCO molecule: the periodical changes of the probability density reflect the stretching and contraction of the iron–carbon bond ($\boldsymbol{R}$) with a vibrational period of about 60 fs.

Here, molecular cations within the electronic ground state [44] and photoelectrons with energy $E_2$ are produced. Fig. 3 contains the time-resolved photoelectron spectrum obtained by the combined interaction of the pump- and probe-pulses. The time-independent contribution centered around an energy $E = E_1$ of 1.34 eV originates in the pump-detachment process. There is, however, a second contribution at larger energies which exhibits a periodic time-dependence. The respective electrons result from the probe-ionization. A comparison to the time-dependent wave packet displayed in Fig. 2 illustrates nicely what was said in Section 2: the transient photoelectron spectrum directly reflects the temporal evolution of the probability density. Thus we are able to take a direct look into the variation of a metal–carbon bond induced by an ultrashort laser pulse.

The example given in this section is of a mere fundamental significance since it shows how, in principle, we are able to map properties of a quantum mechanical wave function onto an observable, i.e. the kinetic energy distribution of photoelectrons. We will now turn to a much more involved photochemical problem where the absorption of several photons by a metal-carbonyl molecule leads to the abstraction of several CO ligands.

## 4. Multiple fragmentation of iron pentacarbonyl

The photochemistry of $Fe(CO)_5$ has been recently investigated by several groups using ultrashort pulses. In these studies a pump–probe ionization detection scheme was used and the signal consisted of the total ion yields $[Fe(CO)_n]^+$ ($n = 0$–5). In the first studies, as carried out by the Gerber group [33,34], the obtained transients were interpreted such as that the absorption of several 400 nm photons leads to fragments which are built on a

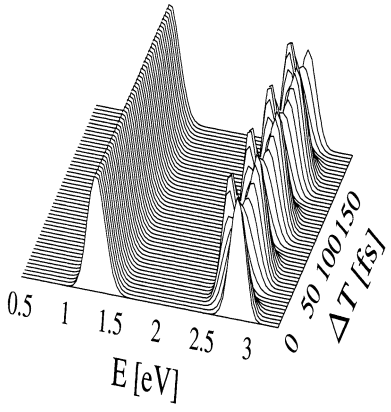


Fig. 3. Time-resolved photoelectron spectrum resulting from a pump-detachment and time-delayed probe-ionization process. The temporal variation of the high energy component reflects the temporal changes of the probability density in Fe–CO as is displayed in Fig. 2.

sub-picosecond time-scale. This interpretation was confirmed by the work of Heinicke and Grotemeyer [37]. However, the sketched multiple fragmentation scenario was not completely accepted within the community: the single-photon experiments, performed with 270 nm pulses by Trushin et al. [38] were interpreted quite differently. In particular, the latter authors concluded that the $FeCO_4$ molecule dissociates within several picoseconds which suggests that what has been measured by Bañares et al. was a dissociation of molecular cations rather than neutral molecules. In fact, these contradictions point to a central difficulty in the interpretation of pump–probe ionization experiments: fragment ions can be obtained by either ionizing neutral fragments of by dissociation of larger cations.

Let us now discuss what will happen if instead of the ion yield, the time-resolved photoelectron spectrum is detected. Rather than going into the theoretical details [47,48], we concentrate on the basic principle in regarding Fig. 4 which displays a pump–probe ionization scheme for a parent molecule (N) (in our case $Fe(CO)_5$ and one fragment (N−1) ($Fe(CO)_4$). The pump-pulse ($\omega_1$) prepares a coherent superposition of eigenstates with energies $E_n$ within the parent molecule. Ionization by the time-delayed second pulse ($\omega_2$) yields a photoelectron distribution centered around a maximum occurring at energy $E$. As was discussed in Section 2, this energy is determined by the difference between the potential energy surfaces of the cationic and neutral electronic state at the mean position of the wave packet serving as initial state for the ionization process. In the figure, the potentials are replaced by the ionization potential $I_N^P$ (which is appropriate if the initial state is a stationary state). The fragmentation now produces fragments with different internal energies $E_{N-1}$. Since the partner fragment takes away a definite amount of energy these energies are lower than the energies $E_N$. The ionization of the fragment (N−1) also produces photoelectrons. However, due to the, in general, different ionization potential (or, more precisely, the different involved potential energy surfaces), the electrons emerge with another distribution of kinetic energies $E'$. Note that although a possible fragmentation of cationic parent molecules might lead to charged fragments, no further photoelectrons can be produced if the laser field strength is weak so that double ionization processes can be neglected. As a consequence, if the ionization potentials $I_N^P$ and $I_{N-1}^P$ differ enough, the time-resolved photoelectron spectrum gives a unique picture of the dissociation in the *neutral* manifold of states.

In our former work [47], we have developed a model which is able to describe the multiple fragmentation of a molecule. The application of this model to the $Fe(CO)_5$ molecule yielded results which are in excellent agreement with the findings of various experiments. In particular we were able to model the transient ion signals as

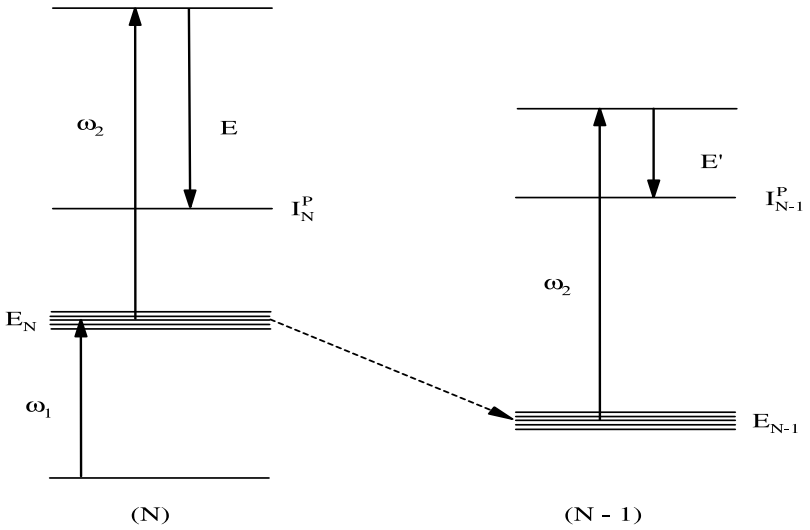


Fig. 4. Time-resolved photoelectron spectrum applied to a fragmentation process. The pump-pulse prepares the parent molecules (N) in excited states with energies $E_N$. The molecule may dissociate leading to a fragment (N−1). Photoinization ($\omega_2$) produces photoelectrons from the parent molecule and the fragment having different kinetic energies $E$ and $E'$.

obtained in the Gerber group [49]. Within the model we calculate the probabilities $g_n(E_n, t)$ to find a particular fragment $Fe(CO)_n$ ($n = 0$–5) with energy $E_n$ at time $t$. In accordance with the interpretation given in Ref. [34], the model assumes a direct $Fe(CO)_5 \rightarrow Fe(CO)_4$ dissociation step (treated as an effective wave-packet motion along a repulsive potential along the reaction coordinate) and indirect subsequent fragmentation processes (treated within the harmonic Slater model [50]). Concerning the photoelectron spectrum, one can show that the spectrum originating from a $Fe(CO)_n$ fragmentation can be approximately written as [48]

$$P_n(E,\ E_n,\ T) \sim g_n(E_n,\ T), \tag{8}$$

subject to the condition

$$\omega_2 - E = I_n^{\mathrm{P}} - E_n. \tag{9}$$

The latter equation defines the resonance condition for ionization and is analogous to Eq. (5) discussed in Section 2. The total spectrum from a single fragment is obtained by integration over the internal energies $E_n$:

$$P_n(E,\ T) = \int \mathrm{d}E_n\ P_n(E,\ E_n,\ T). \tag{10}$$

The time-resolved photoelectron spectra $P_n(E, T)$ as calculated within our simplified model are displayed in Fig. 5. The different panels display contour lines of the spectra obtained from the various fragments. Here we used a pump wavelength of 260 nm. Single photon absorption can lead to $Fe(CO)_n$ ($n = 2$–4) fragments. Smaller fragments are not found since within each dissociation step the CO-fragment takes away energy. Thus, upon dissociation of three CO molecules, $Fe(CO)_2$ is produced with an energy below the threshold for a further break-up. The probe wavelength was set to 130 nm and and the temporal width of both pulses was fixed

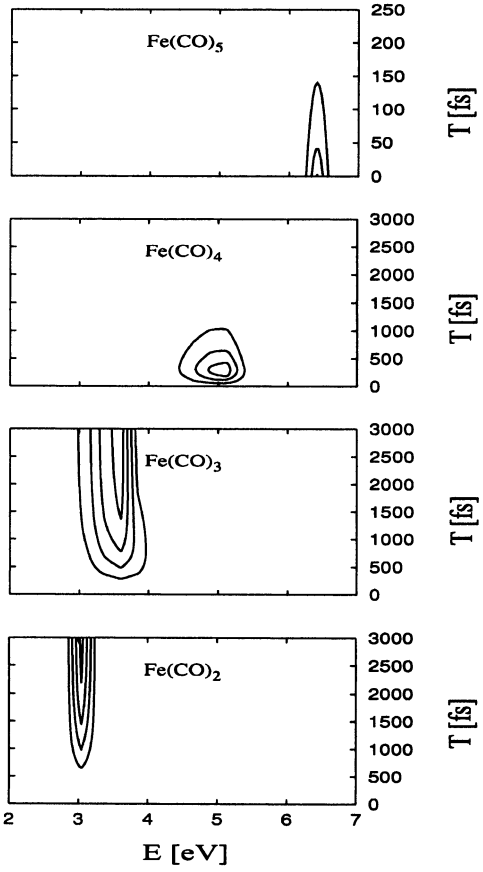


Fig. 5. Contour plots of time-resolved photoelectron spectra from $Fe(CO)_n$ molecules, as indicated. The respective contributions separate on the energy scale (see Fig. 4) so that they can be identified as to originate from the various fragments.

to be 120 fs. The figure illustrates that the initial fragmentation step is finished within the interaction time of the pump-pulse with the molecule (note the different time-scale in the upper panel). The $n = 4$ fragment is built and decays within a picosecond. Simultaneously, $Fe(CO)_3$ molecules are produced which can decompose only partly into $Fe(CO)_2$ and CO. There has been an ongoing discussion if the fragmentation of $Fe(CO)_5$ proceeds sequential or concerted. As mentioned, all CO molecules leave the parent molecule on an ultrashort time-scale so that (within our model) there is no evidence for intermediates with longer lifetimes. This is supported by the measurments of the Gerber group [34] and we may conclude that the fragmentation can be characterized as a concerted process.

Fig. 5 demonstrates that the spectra as obtained from the various molecules clearly separate on the energy scale. This allows for an interpretation of the neutral fragmentation processes. Naturally, since we do not know the involved potential energy surfaces, the distinct features of the total spectrum (consisting of the sum of all $P_n(E, T)$) may be washed out. Nevertheless, as a central result, the calculations illustrate the potential of TRPES in obtaining a detailed view of multiple fragmentation processes. In more detail, the measurement of a transient electron distribution from $Fe(CO)_5$ and its fragments may settle the long standing question if sequential or simultaneous ligand abstraction is the pre-dominant dissociation mechanism.

## 5. Summary

The present paper explores the abilities of time-resolved photoelectron spectroscopy in order to investigate structural changes and photochemical processes occurring in iron carbonyls. In the first example we showed how iron–carbon bond length variations can be observed directly in the electron spectrum. Although a simplified model was used, the principle of the measurement carries over to systems with many internal degrees-of-freedom. Our second example was the photochemical decay of iron pentacarbonyl. The questions to be answered here are: on which time-scale does the multiple Fe–CO bond cleavage occur, does the fragmentation take place in the ionic or neutral channels, and is there a sequential or simultaneous production of CO ligands? Whereas pump–probe measurements of ionic fragments cannot uniquely answer these questions, the detection of time- and energy-resolved photoelectrons allows for a complete characterization of the neutral fragmentation processes. The latter experiment has yet to be performed and might be realized soon [51]. We are confident, that in the near future time-resolved photoelectron spectroscopy will be applied to answer other questions concerning the structure and photoinduced reactions of organometallic compounds.

## Acknowledgements

We gratefully acknowledge support by the Deutsche Forschungsgemeinschaft within the SFB 347 (TP C-5) and the Fonds der Chemischen Industrie.

## References

[1] D.W. Turner, C. Baker, A.D. Baker, C.R. Bundle, Molecular Photoelectron Spectroscopy, Wiley, New York, 1970.
[2] S. Hüfner, Photoelectron Spectroscopy, Springer, Berlin, 1988.
[3] L.V. Azaroff, X-ray Spectroscopy, McGraw-Hill, New York, 1974.
[4] L.S. Cederbaum, J. Zobeley, F. Tarantelli, Phys. Rev. Lett. 79 (1997) 4778.
[5] J. Manz, L. Wöste (Eds.), Femtosecond Chemistry, Wiley-VCH, Weinheim, 1995.
[6] A.H. Zewail, Femtochemistry, World Scientific, Singapore, 1994.
[7] A.H. Zewail, Angew. Chem. Int. Ed. Engl. 39 (2000) 2586.
[8] F.C. De Schryver, S. DeFeyter, G. Schweitzer (Eds.), Femtochemistry, Wiley-VCH, Weinheim, 2001.
[9] A.H. Zewail, Science 242 (1988) 1645.
[10] M. Seel, W. Domcke, Chem. Phys. 151 (1991) 59.
[11] M. Seel, W. Domcke, J. Chem. Phys. 95 (1991) 7806.
[12] D.R. Cyr, C.C. Hayden, J. Chem. Phys. 104 (1996) 771.
[13] A. Assion, M. Geisler, J. Helbing, V. Seyfried, T. Baumert, Phys. Rev. A 54 (1996) R4605.
[14] B.J. Greenblatt, M.T. Zanni, D.M. Neumark, Chem. Phys. Lett. 258 (1996) 523.
[15] P. Ludowise, M. Blackwell, Y. Chen, Chem. Phys. Lett. 258 (1996) 530.
[16] C. Jouvet, S. Martrenchard, D. Solgadi, C. Dedonder-Lardeux, M. Mons, G. Grégoire, I. Dimicoli, F. Piuzzi, J.P. Visticot, J.M. Mestdagh, P. D'Oliveira, P. Meynadier, M. Perdrix, J. Phys. Chem. Sect. A 101 (1997) 2555.
[17] V. Blanchet, A. Stolow, J. Chem. Phys. 108 (1998) 4371.
[18] J.A. Davies, J.E. LeClaire, R.E. Continetti, C.C. Hayden, J. Chem. Phys. 111 (1999) 1.
[19] P. Farmanara, W. Radloff, V. Stert, H.-H. Ritze, I.V. Hertel, J. Chem. Phys. 111 (1999) 633.
[20] T. Frohnmeyer, M. Hofmann, M. Strehle, T. Baumert, Chem. Phys. Lett. 312 (1999) 447.
[21] S. Lochbrunner, T. Schultz, M. Schmitt, J.P. Shaffer, M.Z. Zgierski, A. Stolow, J. Chem. Phys. 114 (2001) 2519.
[22] V. Stert, P. Farmanara, H.-H. Ritze, W. Radloff, K. Gasmi, A. Gonzalez-Urena, Chem. Phys. Lett. 337 (2001) 299.
[23] T. Suzuki, L. Wang, H. Kohguchi, J. Chem. Phys. 111 (1999) 4859.
[24] J.A. Davies, R.E. Continetti, D.W. Chandler, C.C. Hayden, Phys. Rev. Lett. 84 (2000) 5983.
[25] M. Tsubouchi, B.J. Whitaker, L. Wang, H. Kohguchi, T. Suzuki, Phys. Rev. Lett. 86 (2001) 4500.
[26] T. Seideman, J. Chem. Phys. 107 (1997) 7859.
[27] T. Seideman, Ann. Rev. Phys. Chem. 53 (2002) 41.
[28] Y. Arasaki, K. Takatsuka, K. Wang, V. McKoy, Chem. Phys. Lett. 302 (1999) 363.
[29] Y. Arasaki, K. Takatsuka, K. Wang, V. McKoy, J. Chem. Phys. 112 (2000) 8871.

[30] S.A. Angel, P.A. Hansen, E.J. Heilweil, J.C. Stephenson, Ultrafast phenomena VII, in: C.B. Harris, E.P. Ippen, G.A. Mourou, A.H. Zewail (Eds.), Springer Series in Chemical Physics, vol. 53, Springer, Berlin, 1990, p. 480.
[31] S.K. Kim, S. Pedersen, A.H. Zewail, Chem. Phys. Lett. 233 (1995) 500.
[32] T. Lian, W.E. Bromberg, M.C. Asplund, H. Yang, C.B. Harris, J. Phys. Chem. 100 (1996) 11994.
[33] L. Bañares, T. Baumert, M. Bergt, B. Kiefer, G. Gerber, Chem. Phys. Lett. 267 (1997) 141.
[34] L. Bañares, T. Baumert, M. Bergt, B. Kiefer, G. Gerber, J. Chem. Phys. 108 (1997) 5799.
[35] M. Gutmann, J.M. Janello, M.S. Dickebohm, M. Grossekathoefer, J. Lindener-Roenneke, J. Phys. Chem. Sect. A 102 (1998) 4138.
[36] M. Gutmann, J.M. Janello, M.S. Dickebohm, Chem. Phys. 239 (1998) 317.
[37] R. Heinicke, J. Grotemeyer, Appl. Phys. B 71 (2000) 419.
[38] S.A. Trushin, W. Fuss, K.L. Kompa, W.E. Schmid, J. Phys. Chem. Sect. A 104 (2000) 1997.
[39] C. Daniel, J. Full, L. González, C. Kaposta, M. Krenz, C. Lupulescu, J. Manz, S. Minemoto, M. Oppel, P. Rosendo-Francisco, Š. Vajda, L. Wöste, Chem. Phys. 267 (2001) 247.
[40] Y. Kasai, K. Obi, Y. Ohshima, Y. Endo, K. Kawaguchi, J. Chem. Phys. 103 (1995) 90.
[41] P.W. Villalta, D.G. Leopold, J. Chem. Phys. 98 (1993) 7730.
[42] K. Tanaka, M. Shirasaka, T. Tanaka, J. Chem. Phys. 106 (1997) 6820.
[43] N.E. Henriksen, V. Engel, Int. Rev. Phys. Chem. 20 (2001) 93.
[44] M. Castro, D.R. Salahub, R. Fournier, J. Chem. Phys. 100 (1994) 8233.
[45] S. Wolf, G. Sommerer, S. Rutz, E. Schreiber, T. Leisner, E. Wöste, R.S. Berry, Phys. Rev. Lett. 74 (1995) 4177.
[46] O. Rubner, C. Meier, V. Engel, J. Chem. Phys. 107 (1997) 1066.
[47] O. Rubner, V. Engel, J. Chem. Phys. 115 (2001) 2936.
[48] M. Erdmann, O. Rubner, Z. Shen, V. Engel, Chem. Phys. Lett. 341 (2001) 338.
[49] O. Rubner, T. Baumert, M. Bergt, B. Kiefer, G. Gerber, V. Engel, Chem. Phys. Lett. 316 (2000) 585.
[50] N.B. Slater, Proc. Camb. Phil. Soc. 35 (1939) 56.
[51] G. Gerber, private communication.